Nontopological soliton in the Polyakov quark-meson model

Jinshuang Jin and Hong Mao*
Department of Physics, Hangzhou Normal University, Hangzhou 310036, China
(Received 24 August 2015; revised manuscript received 18 November 2015; published 7 January 2016)

Within a mean-field approximation, we study a nontopological soliton solution of the Polyakov quark-meson model in the presence of a fermionic vacuum term with two flavors at finite temperature and density. The profile of the effective potential exhibits a stable soliton solution below a critical temperature $T \leqslant T_\chi^c$ for both the crossover and the first-order phase transitions, and these solutions are calculated here with appropriate boundary conditions. However, it is found that only if $T \leqslant T_d^c$ is the energy of the soliton M_N less than the energy of the three free constituent quarks $3M_q$. As $T > T_d^c$, there is an instant delocalization phase transition from hadron matter to quark matter. The phase diagram together with the location of a critical end point has been obtained in the T and μ plane. We notice that two critical temperatures always satisfy $T_d^c \leqslant T_\chi^c$. Finally, we present and compare the result of thermodynamic pressure at zero chemical potential with lattice data.

DOI: 10.1103/PhysRevC.93.015202

I. INTRODUCTION

It is widely believed that at sufficiently high temperatures and densities there is a quantum chromodynamics (QCD) phase transition between normal nuclear matter and quark-gluon plasma (QGP), where quarks and gluons are no longer confined in hadrons [1,2]. The study of the QCD phase transition is experimentally supported by the heavy-ion collisions at ultrarelativistic energies, accomplished in the most sophisticated accelerators, such as the Relativistic Heavy Ion Collider at Brookhaven National Laboratory and the Large Hadron Collider at CERN. These conducted experiments provide us with the opportunity to infer fundamental information about which type phase of matter, hadronic or quark-gluon plasma, is stabilized in the various regimes. To explore a wider range of the QCD phase transition up to several times the normal nuclear-matter density, the new Facility for Antiproton and Ion Research at Darmstadt, the Nuclotron-based Ion Collider Facility at the Joint Institute for Nuclear Research in Dubna, and the Japan Proton Accelerator Research Complex at Japan Atomic Energy Research Institute and Japan's National Laboratory for High Energy Physics will make such extreme conditions possible through collisions [3]. Therefore, it will be possible to test the theoretical predictions about the hadron-quark phase transition at high density but moderate temperature.

On the theoretical side, the property of confinement which becomes relevant at large distances or equivalently low energies has hindered the development of analytical and numerical methods capable of describing the low-energy nonperturbative cases, especially if baryons are involved. Therefore, the challenge for nuclear physicists remains to find models that can bridge the gap between the fundamental theory and our wealth of knowledge about low-energy phenomenology. Moreover, these models should be successful in explaining empirical facts at low energies, for example, the dynamical breaking of chiral symmetry and the confinement, which are both intimately related to the nonperturbative structure of the QCD vacuum. To mention a few, these effective models are the MIT bag model [4], the Nambu-Jona-Lasinio (NJL) [5,6], and the linear σ model [7] for quark matter, while others are the Brueckner-Hartree-Fock (BHF) theory [8] and the relativistic mean-field (RMF) models [9] for nuclear matter.

Because the strongly interacting matter at very high energy should have quarks and gluons as the degrees of freedom, while nucleons and mesons are the relevant degrees of freedom in the hadron phase. On one hand, the phenomenology of the hadron-quark phase transition is often studied with the above-mentioned effective models [10–12], where the BHF theory including the realistic baryon baryon interaction or the RMF models is used to describe hadron phase, while on the other hand, the quark phase is treated as a thermodynamic bag model or simulated by the NJL model [or its modernized version, the Polyakov-Nambu-Jona-Lasinio (PNJL) model] [13]. The motivation for these studies, aims at rendering two models with different degrees of freedom compatible. In more detail, the MIT bag model and PNJL models do describe the very well-known properties of quark matter, but they fail to reproduce the bulk nuclear matter and finite nuclei properties. However, the BHF theory and the RMF models which are constructed for nuclear matter are often questionable when extending to investigate high-density regimes as it is common for neutron stars. Then the approach of considering the mixed phase of hadron and quark matter becomes important, and the proper equation of state for the hadron-quark phase transition could be derived based on the Gibbs conditions for phase equilibrium. Unfortunately, this kind of study is applicable only if the QCD phase transition is of first order. According to a recent study on the QCD phase diagram based on chiral effective models, including quark and meson fluctuations via the functional renormalization group [14], the biggest part of the QCD phase diagram shows crossover transitions rather than true first-order ones. Thus, it is necessary to search for an alternative effective model which can provide a proper description of hadron-quark phase transition beyond the first-order transition cases, including the crossover situations, while keeping at the same time the correct degrees of freedom in quark phase and

*Corresponding author: mao@hznu.edu.cn

hadron phase intact. The nontopological soliton model rooted on the Polyakov quark-meson model [15] appears to fulfill the requirement.

The Polyakov quark-meson model has so far facilitated the investigation of the full QCD thermodynamics and phase structure at zero and finite quark chemical potential, while it has been shown that the bulk thermodynamic predictions of the model agree well with the lattice QCD data [14–23]. However, starting from the same Lagrangian, bound states (solitons) of valence quarks can be constructed through the interaction with σ and π mesons [24,25]. Such a nontopological soliton gives rise to nucleons in the hadron phase. Moreover, the nontopological soliton model has been proven to be a successful approach for the description of the static properties of nucleons in vacuum [24,26–30]. Combining these two features together, while also requiring a soliton embedded in a thermal medium, the model provides a suitable working scheme to simultaneously study both the restoration of chiral symmetry and the possible dissolution of the soliton, which simulates the deconfinement transition of nuclear matter to quark matter.

In fact, the nucleon has been previously investigated in Ref. [31] by employing the chiral soliton model and viewing it as a $B = 1$ chiral soliton in a cold quark medium. However, the parameters f_π, m_π, and m_σ were chosen to be the medium-modified meson values within the NJL model. For finite temperature, Abu-Shady and Mansour have studied nucleon properties [32] by employing the one-loop phenomenological mesonic potential [33] and the coherent-pair approximation [29,30]. Furthermore, the nucleon properties as well as the thermodynamics of the system both at finite temperature and density are examined in Refs. [34–36]. However, these studies based on the chiral soliton model or other nontopological soliton models [37–40] suffer from two problems: The one is that they only predict a first-order phase transition and the other is that the critical temperature is extremely low ($T_c \sim 110$ MeV) as compared with lattice data. In this work, we improve these previous studies by combing the chiral soliton model with the Polyakov-loop field. Such an extension will allow us to inspect both the crossover and first-order QCD phase transitions and compare directly with the lattice QCD simulations.

The structure of the paper is as follows. In the next section we introduce the Polyakov-quark-meson model with two quark flavors. In Sec. III, after obtaining the effective potential in the mean-field approximation, we explore the possible stable soliton solutions in the model. Section IV is devoted to derive the equations of motion of the nontopological soliton model both in vacuum and at finite temperature and density. Section V contains the static properties of nucleon at finite temperature and density and the phase diagram at the T-μ plane. The study of the hadron-quark phase transition is presented in Sec. VI. We conclude with a summary and discussions in Sec. VII.

II. THE MODEL

We work in a generalized Lagrangian of the quark-meson model for $N_f = 2$ quarks and $N_c = 3$ color degrees with quarks coupled to a spatially constant time-dependent background gauge field representing Polyakov-loop dynamics (the Polyakov-quark-meson model or the PQM in short). The Lagrangian reads [15]

$$\mathcal{L} = \overline{\psi}[i\gamma^\mu D_\mu - g(\sigma + i\gamma_5\vec{\tau}\cdot\vec{\pi})]\psi + \tfrac{1}{2}(\partial_\mu\sigma\partial^\mu\sigma + \partial_\mu\vec{\pi}\cdot\partial^\mu\vec{\pi}) - U(\sigma,\vec{\pi}) - \mathcal{U}(\Phi,\Phi^*,T). \tag{1}$$

Here we have introduced a flavor-blind Yukawa interaction of strength g, coupling the isodoublet spin-$\frac{1}{2}$ quark fields $\psi = (u,d)$ with the spin-0 isosinglet σ and the isotriplet pion field $\vec{\pi} = (\pi_1,\pi_2,\pi_3)$. In addition, there exists a spatially homogeneous time-dependent gauge field represented by the Polyakov-loop potential. The coupling of the quarks with the uniform temporal background gauge field is implemented through the covariant derivative $D_\mu = \partial_\mu - iA_\mu$ and the spatial components of the gauge fields have vanishing background $A_\mu = \delta_{\mu 0}A_0$.

The purely mesonic potential for the σ and $\vec{\pi}$ is defined as

$$U(\sigma,\vec{\pi}) = \frac{\lambda}{4}(\sigma^2 + \vec{\pi}^2 - \vartheta^2)^2 - H\sigma - \frac{m_\pi^4}{4\lambda} + f_\pi^2 m_\pi^2, \tag{2}$$

and the minimum energy occurs for chiral fields σ and $\vec{\pi}$ restricted to the chiral circle in the physical vacuum,

$$\sigma^2 + \vec{\pi}^2 = f_\pi^2, \tag{3}$$

where $f_\pi = 93$ MeV, corresponds to the pion decay constant and $m_\pi = 138$ MeV is the pion mass. The last two constant terms in Eq. (2) are used to guarantee that the energy of the vacuum in the absence of quarks is zero. The constant H is fixed by the partially conserved axial-vector current relation, which gives $H = f_\pi m_\pi^2$.

The quantity $\mathcal{U}(\Phi,\Phi^*,T)$ is the Polyakov-loop effective potential. The Polyakov-loop field Φ is defined as the thermal expectation value of the color trace of the Wilson loop along the temporal direction,

$$\Phi = (\mathrm{Tr}_c L)/N_c, \quad \Phi^* = (\mathrm{Tr}_c L^\dagger)/N_c. \tag{4}$$

The Polyakov loop L is a matrix in color space and explicitly given by

$$L(\vec{x}) = \mathcal{P}\exp\left[i\int_0^\beta d\tau A_4(\vec{x},\tau)\right], \tag{5}$$

with $\beta = 1/T$ being the inverse of temperature and $A_4 = iA^0$. In the so-called Polyakov gauge, the Polyakov-loop matrix can be given as a diagonal representation [41]. Within this diagonal representation, Φ and Φ^* are complex scalar fields. Their mean values are related to the free energy of a static, infinitely heavy test quark (antiquark) at spatial position $\vec{x}$. The Polyakov-loop expectation value $\langle\Phi\rangle$ vanishes in the confined phase where the free energy of a single heavy quark diverges, while in the deconfined phase it takes a finite value because the center symmetry becomes spontaneously broken [42].

The temperature-dependent effective potential $\mathcal{U}(\Phi,\Phi^*,T)$ is constructed to reproduce the thermodynamical behavior of the Polyakov loop for the pure gauge case in accordance with lattice QCD data, and it has the $Z(3)$ center symmetry like the pure gauge QCD Lagrangian. In the absence of quarks, we have $\Phi = \Phi^*$ and the Polyakov loop is taken as an order parameter

for deconfinement. For low temperatures, $\mathcal{U}$ has a single minimum at $\Phi = 0$, while at high temperatures it develops a second one which turns into the absolute minimum above a critical temperature T_0 and the $Z(3)$ center symmetry is spontaneously broken. The simplest $Z(3)$ symmetric polynomial form based on a Ginzburg-Landau ansatz is proposed in Ref. [43],

$$\frac{\mathcal{U}(\Phi,\Phi^*,T)}{T^4} = -\frac{b_2(T)}{4}(|\Phi|^2+|\Phi^*|^2) - \frac{b_3}{6}(\Phi^3+\Phi^{*3}) + \frac{b_4}{16}(|\Phi|^2+|\Phi^*|^2)^2, \tag{6}$$

with

$$b_2(T) = a_0 + a_1\left(\frac{T_0}{T}\right) + a_2\left(\frac{T_0}{T}\right)^2 + a_3\left(\frac{T_0}{T}\right)^3. \tag{7}$$

A precise fit of the constants a_i,b_i is performed to reproduce the lattice data for the pure gauge theory thermodynamics, as also the behavior of the Polyakov loop as a function of temperature. The corresponding parameters are

$$\begin{aligned} &a_0 = 6.75, \quad a_1 = -1.95, \quad a_2 = 2.625, \\ &a_3 = -7.44, \quad b_3 = 0.75, \quad b_4 = 7.5. \end{aligned} \tag{8}$$

Originally, the critical temperature T_0 for deconfinement in the pure gauge sector is fixed at 270 MeV, in agreement with the lattice results. However, in fully dynamical QCD, fermionic contributions and the matter backreaction modify the pure gauge potential to an effective glue potential, which carries a flavor and chemical potential dependence of T_0. The actual value of T_0 for two quark flavors is $T_0 = 208$ MeV [15,18].

A convenient framework of studying phase transitions is the thermal field theory. Within this framework, the finite-temperature effective potential is an important and useful theoretical tool. In this section, to investigate the temperature and the chemical potential dependence of the nontopological soliton, let us consider a spatially uniform system in thermodynamical equilibrium at temperature T and quark chemical potential μ. In general, the grand partition function reads

$$\begin{aligned} \mathcal{Z} &= \mathrm{Tr}\exp[-(\hat{\mathcal{H}} - \mu\hat{\mathcal{N}})/T] \\ &= \int\prod_a \mathcal{D}\sigma\mathcal{D}\pi_a \int \mathcal{D}\psi\mathcal{D}\bar{\psi}\exp\left[\int_x(\mathcal{L}+\mu\bar{\psi}\gamma^0\psi)\right], \end{aligned} \tag{9}$$

where $\int_x \equiv i\int_0^{1/T} dt \int_V d^3x$, V is the volume of the system, and $\mu = \mu_B/3$ for the homogeneous background field.

We evaluate the partition function in the mean-field approximation similar to the work of Ref. [44]. Thus, we replace the meson fields with their expectation values in the action. In other words, we neglect both quantum and thermal fluctuations of the meson fields. The quarks and antiquarks are retained as quantum fields. The integration over the fermions yields a determinant which can be calculated by standard methods [45]. This generates an effective potential for the mesons. Finally, we obtain the thermodynamical potential density as

$$\Omega(T,\mu) = \frac{-T\ln\mathcal{Z}}{V} = U(\sigma,\vec{\pi}) + \mathcal{U}(\Phi,\Phi^*,T) + \Omega_{\bar{\psi}\psi}, \tag{10}$$

with the quarks and antiquarks contribution

$$\begin{aligned} \Omega_{\bar{\psi}\psi} &= \Omega^{\mathrm{v}}_{\bar{\psi}\psi} + \Omega^{\mathrm{th}}_{\bar{\psi}\psi} \\ &= -2N_fN_c\int\frac{d^3\vec{p}}{(2\pi)^3}E_q \\ &\quad - 2N_fT\int\frac{d^3\vec{p}}{(2\pi)^3}[\ln g_q^+ + \ln g_q^-], \end{aligned} \tag{11}$$

where, $N_f = 2$, $N_c = 3$, and $E_q = \sqrt{\vec{p}^2 + M_q^2}$ is the valence quark and antiquark energy for u and d quarks, and the constituent quark (antiquark) mass M_q is defined as $M_q = g\sigma_v$ together with $\sigma_v \equiv \sqrt{\sigma^2+\vec{\pi}^2}$. The first term of Eq. (11) denotes the fermion vacuum one-loop contribution, regularized by the ultraviolet cutoff. In the second term g_q^+ and g_q^- are defined as taking trace over color space:

$$g_q^+ = [1 + 3(\Phi + \Phi^* e^{-(E_q-\mu)/T})\times e^{-(E_q-\mu)/T} + e^{-3(E_q-\mu)/T}], \tag{12}$$

$$g_q^- = [1 + 3(\Phi^* + \Phi e^{-(E_q+\mu)/T})\times e^{-(E_q+\mu)/T} + e^{-3(E_q+\mu)/T}]. \tag{13}$$

The fermion vacuum one-loop contribution $\Omega^{\mathrm{v}}_{\bar{\psi}\psi}$ is frequently omitted. In this work, we include the effect of vacuum fluctuation on the thermodynamics. This term can be properly renormalized by using the dimensional regularization scheme as done for the two-flavor case in Refs. [18–20], and the renormalized contribution of the fermion vacuum loop reads

$$\Omega^{\mathrm{v}}_{\bar{\psi}\psi} = \Omega^{\mathrm{reg}}_{\bar{\psi}\psi} = -\frac{N_cN_f}{8\pi^2}M_q^4\ln\left(\frac{M_q}{\Lambda}\right), \tag{14}$$

where Λ is the arbitrary renormalization scale. It is worth noting that the thermodynamic potential and all physical observable are independent of the choice of Λ, and the Λ dependence can be neatly canceled out by redefining the parameters in the model.

Now the first term in the right-hand side of Eq. (11), describing the vacuum contribution, is replaced with the appropriately renormalized fermion vacuum contribution as given in Eq. (14). Accordingly, the thermodynamic grand potential in the presence of appropriately renormalized fermionic vacuum contribution in the Polyakov quark-meson model is written as

$$\Omega_{\mathrm{MF}}(T,\mu,\sigma_v,\Phi,\Phi^*) = \Omega_{\mathrm{M}}(\sigma_v) + \mathcal{U}(\Phi,\Phi^*,T) + \Omega^{\mathrm{th}}_{\bar{\psi}\psi}. \tag{15}$$

Here, for convenience, we define a new mesonic potential,

$$\Omega_{\mathrm{M}}(\sigma_v) = U(\sigma,\vec{\pi}) + \Omega^{\mathrm{reg}}_{\bar{\psi}\psi}, \tag{16}$$

which is independent of the temperature T and the chemical potential μ. Minimizing the thermodynamical potential in Eq. (15) respective to σ_v, Φ, and Φ^*, we obtain a set of equations of motion:

$$\frac{\partial\Omega_{\mathrm{MF}}}{\partial\sigma_v} = 0, \quad \frac{\partial\Omega_{\mathrm{MF}}}{\partial\Phi} = 0, \quad \frac{\partial\Omega_{\mathrm{MF}}}{\partial\Phi^*} = 0. \tag{17}$$

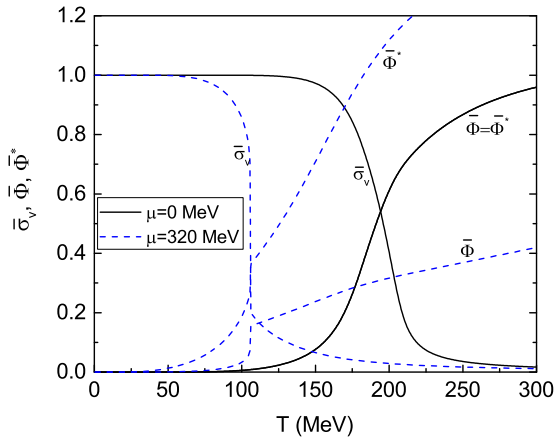

FIG. 1. The normalized chiral order parameter $\bar{\sigma}_v$ and the Polyakov-loop expectation values $\bar{\Phi}$, $\bar{\Phi}^*$ as functions of temperature for $\mu = 0$ MeV and $\mu = 320$ MeV. The solid curves are for $\mu = 0$ MeV and the dashed curves are for $\mu = 320$ MeV.

The set of equations can be solved for the fields as functions of temperature T and chemical potential μ, and the solutions of these coupled equations determine the behavior of the chiral order parameter $\bar{\sigma}_v$ and the Polyakov-loop expectation values $\bar{\Phi}$, $\bar{\Phi}^*$ as a function of T and μ.

There are two values of the constants left in the model which we need to fix, namely, m_σ and g. Unlike the pion meson, the mass of the σ meson still has a poorly known value, but the most recent result of the Particle Data Group considers that m_σ can vary from 400 to 550 MeV with full width 400–700 MeV [46]. The coupling constant g is usually fixed by the constituent quark mass in vacuum within the range of 300–500 MeV, which gives $g \simeq 3.3$–5.3. In this work we take $m_\sigma = 472$ MeV and $g = 4.5$ as the typical values. It has been proved in Ref. [34] that this set of parameters can describe the properties of nucleon in vacuum successfully.

In Fig. 1, the temperature dependence of the normalized chiral order parameter $\bar{\sigma}_v$ and the Polyakov-loop expectation values $\bar{\Phi}$, $\bar{\Phi}^*$ at $\mu = 0$ MeV and $\mu = 320$ MeV are shown in relative units. The temperature behaviors of the chiral condensate and Polyakov loop condensate show that the system experiences a smooth crossover transition at zero chemical potential, while there is a first-order phase transition for larger chemical potential because both the chiral order parameter and the Polyakov-loop expectation values make jumps across the gap of the condensates near the critical temperature. Traditionally, the temperature derivative of the chiral condensate $\bar{\sigma}_v$ for u and d quarks has a peak at some specific temperature, which is established as the critical temperature for the chiral phase transition for both the crossover and the first-order transitions. Thus, for zero chemical potential, the chiral restoration occurs at $T_\chi^c \simeq 201$ MeV, whereas for a relatively larger chemical potential $\mu = 320$ MeV, the critical temperature moves to the lower temperature region around $T_\chi^c \simeq 105$ MeV.

Although different from the chiral phase transition, we are still not in a position to conclusively identify the deconfinement phase transition through the Polyakov loop expectation values $\bar{\Phi}$, $\bar{\Phi}^*$ or their temperature derivatives [21,47]. The temperature derivatives $\bar{\Phi}'$ and $\bar{\Phi}^{*\prime}$ do show one peak or more peaks for zero chemical potential or finite chemical potentials in calculations, but unfortunately these peaks are fake signals for defining the critical temperature of the deconfinement. In the next section, based on the effective potential at finite temperature and finite chemical potential, we explain that there is no obvious clue to define the critical temperature of the deconfinement phase transition simply by using the Polyakov-loop expectation values $\bar{\Phi}$, $\bar{\Phi}^*$ or their temperature derivatives if $T < T_0$, even in the first-order transition region. This is a serious problem which appeared already in the Polyakov quark-meson model [15,21] or the PNJL model [41,47] and still persists in more recent theories. In the following, based on the nontopological soliton model, we provide a distinct clarification on this point which will allow us to propose a convincing definition of the deconfinement critical temperature.

III. EFFECTIVE POTENTIAL AND NONTOPOLOGICAL SOLITON

The basic ideas behind the nontopological soliton are best illustrated by considering the original model: the Friedberg-Lee model [48] or its descendant models [24,25,49]. In these models, the confinement of quarks is approximated through their interaction with the phenomenological scalar field, σ, which is introduced to describe the complicated nonperturbative features of the QCD vacuum. In mean-field approximation, the σ field has a baglike soliton solution, named as a nontopological soliton. This is in contrast to topological defects which are stabilized by the topological properties of the vacuum manifold. The existence of this kind of solution is closely related to a potential describing the nonlinear self-interactions of the σ field. In general, the potential leading to the soliton solution has three extrema: one local minimum corresponding to a perturbative vacuum state located at $\sigma \simeq 0$, one absolute minimum corresponding to a physical vacuum at its vacuum value $\bar{\sigma}_v$, and a local maximum lying between 0 and $\bar{\sigma}_v$. Therefore, the soliton solution has a spherical cavitylike structure: At large radius r, the σ field assumes its vacuum value σ_v, but at small r, the σ field has a value close to the second minimum of the potential near zero. In the Friedberg-Lee model the quarks interact with a mean σ field only; this means that in the physical vacuum state the quark mass is more than 1 GeV, which makes it energetically unfavorable for the quark to exist freely, so that the effective heavy quarks have to be confined in hadron bags. Sometimes it is also called as "absolute" confinement, similar to the MIT bag model. However, as it is known for the chiral soliton model, pions can produce strongly attractive forces among the quarks. Including mean pion fields also allows the meson fields to remain close to the minimum of the Mexican hat potential, and so quarks possess physical constituent masses in the physical vacuum. The state is to be bound if only the total energy of system is lower than the energy of three free constituent quarks in the system, making it thus transparent for considering the chiral soliton as a bound state in this work.

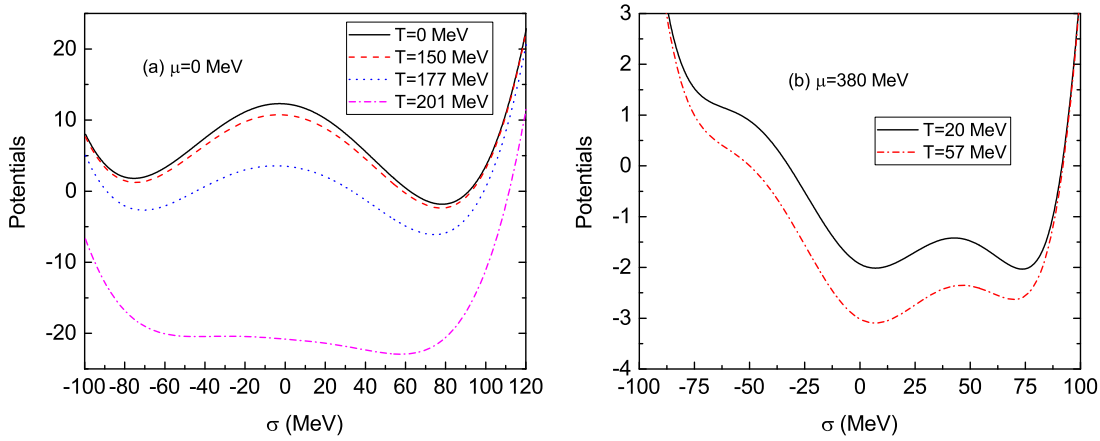

FIG. 2. (a) The grand-canonical potentials $\Omega_{\rm MF}$ as a function of the chiral order parameter σ for $\mu = 0$ MeV by fixing the Polyakov loop on their expectation values. (b) The grand-canonical potentials $\Omega_{\rm MF}$ as a function of the chiral order parameter σ for $\mu = 380$ MeV by fixing the Polyakov loop on their expectation values. $\Omega_{\rm MF}$ is scaled by a factor of f_π^4.

Normally, the self-interaction potential of the σ field is chosen to have a quartic form in the nontopological soliton model, and the coefficients in the quartic potential can be chosen so that they belong to the three typical forms as described in a seminal work done by Goldflam and Wilets [50]. In their work, they have shown that to ensure the stability of the two vacuum states and guarantee the existence of the stable soliton solution, it is indispensable for the potential of the σ field to exhibit three distinct extrema. In the following discussion, this is also considered as a key criterion for determining whether there exist stable soliton solutions for the mesonic fields and the Polyakov-loop fields. Then with employing the thermodynamic grand potential in the presence of appropriately renormalized fermionic vacuum contribution in Eq. (15), we can explore the possible nontopological soliton solutions owned by the model under this criterion.

However, in contrast to the chiral soliton and the Friedberg-Lee models, in the present study there are three order parameter variables σ_v, Φ, and Φ^* in the grand-canonical potential $\Omega_{\rm MF}$ in Eq. (15), so it is extremely difficult to investigate and demonstrate the effective potential at finite temperature and chemical potential via evolving these variables simultaneously in such a large parameter space. To simplify the problem and provide a more intuitive insight into the physics, we separate the study into two cases: (1) the mesonic field direction and (2) the Polyakov-loop field direction. For the first case, we treat the σ field as a variable in the grand-canonical potential $\Omega_{\rm MF}$ while fixing the Polyakov-loop fields on their expectation values $\bar{\Phi}$ and $\bar{\Phi}^*$. In contrast, for the second case, the Polyakov loops Φ and Φ^* are considered as variables, while the σ field maintains its expectation value $\bar{\sigma}_v$ all the time.

The first case is shown in Fig. 2, where the left panel is for zero chemical potential and the right panel for $\mu = 380$ MeV. Here the expectation value of the pion field is chosen in the standard way as $\langle\vec{\pi}\rangle = 0$. For $\mu = 0$ MeV, one clearly observes a smooth crossover of the symmetry-breaking pattern. The energy difference $\Delta\varepsilon$ between the global minimum and the local maximum of the potential decreases upon the increase of the temperatures. When a critical temperature $T_\chi^c \simeq 201$ MeV is reached, $\Delta\varepsilon$ vanishes, which indicates that the chiral symmetry is restored. Moreover, according to the above criterion for the existence of the stable soliton solution, for zero chemical potential, we can find the stable soliton solutions at various temperature from zero temperature to the critical temperature for the chiral phase transition T_χ^c. The result is believed to be held for all crossover transition regions in the QCD phase diagram.

For $\mu = 380$ MeV, one clearly observes the characteristic pattern of a first-order phase transition: Two minima corresponding to phases of restored and broken symmetry are separated by a potential barrier and they will become degenerate at $T = T_\chi^c$. Chiral symmetry is approximately restored for $T > T_\chi^c$, where the minimum at perturbative vacuum $\sigma \sim 0$ becomes the absolute minimum, as shown in the right panel in Fig. 2. The bag constant B is now negative; then it is physically prohibited to support the existence of the stable soliton solution, so that there is no soliton solution anymore. Therefore, we can only obtain the stable soliton solution for $T \leqslant T_\chi^c$, and this is also applicable for the whole first-order transition region in the QCD phase diagram. Moreover, the barrier between the two local minima of the effective potential around T_χ^c, shown in the right panel in Fig. 2, will decrease with decreasing μ. At a specific chemical potential, μ^c, the barrier will finally disappear and the transition will become of second order. The point C (T_χ^c, μ^c) of the phase diagram is termed as the critical end point (CEP).

Let us now investigate how the grand-canonical potentials $\Omega_{\rm MF}$ evolve with the Polyakov-loop field Φ for different chemical potentials by fixing the chiral order parameters on their expectation values. The scaled grand-canonical potential is shown in Fig. 3 as a function of Φ. From Fig. 3 it is obvious that these effective potentials share similar behaviors for both $\mu = 0$ MeV and $\mu = 380$ MeV: There is only one minimum for each of the effective potentials, and these minima correspond to the expectation values $\bar{\Phi}$ of the Polyakov-loop field at specific temperature and density. In the crossover transition region, with the raising of the temperature, the expectation value $\bar{\Phi}$ moves to its higher value smoothly and

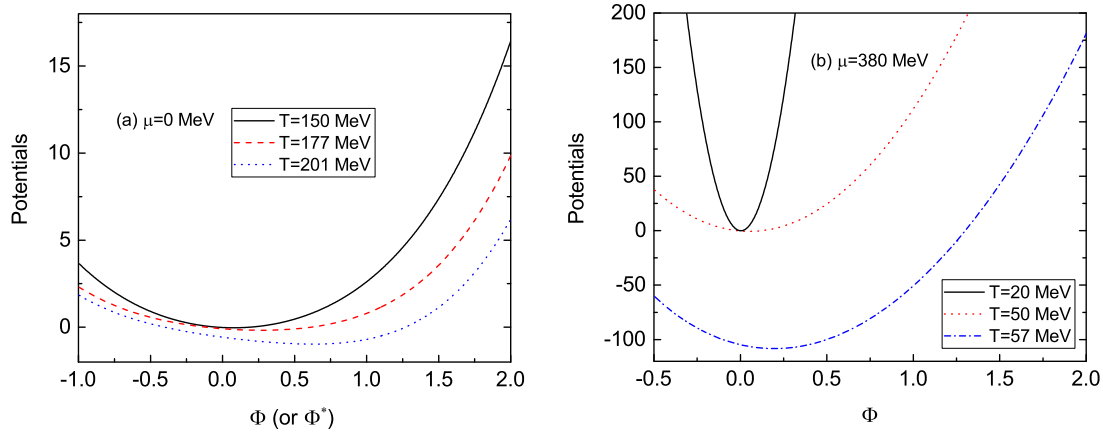

FIG. 3. (a) The grand-canonical potential $\Omega_{\rm MF}$ as a function of the Polyakov loop Φ (or Φ^*) for $\mu = 0$ MeV by fixing the chiral order parameters on their expectation values. (b) The grand-canonical potential $\Omega_{\rm MF}$ as a function of the Polyakov loop Φ for $\mu = 380$ MeV by fixing the chiral order parameter on their expectation values. $\Omega_{\rm MF}$ is scaled by a factor of T^4.

slowly. However, in the first-order transition region at high density, accompanied by the jump of chiral order parameter σ, the expectation value $\bar{\Phi}$ develops a disconnection across the gap from relatively small value to its maximum, which indicates that there exists a degenerate value of the Polyakov-loop variable Φ along the first-order transition line in the QCD phase diagram for very high chemical potential. This implies that the integration of the quark and meson fields in the grand-canonical potential $\Omega_{\rm MF}$ would only result in a trivial Polyakov-loop effective potential at finite T and μ, and such a naive potential does not tell anything about the critical point at which the deconfinement transition should definitely happened. Therefore, the jump induced by the chiral order parameter is not to be supported by the effective potential of the Polyakov-loop field itself; then it certainly cannot be treated as a signal for the deconfinement phase transition. This is the reason why we argue that there exists no obvious criterion for defining the critical temperature for the deconfinement phase transition in terms of using the Polyakov-loop variables Φ, Φ^* or their temperature derivatives, as long as the temperature T is smaller than the critical temperature T_0 for deconfinement in the pure gauge sector.

Nevertheless, the advantage is that we do not have a baglike soliton solutions for the Polyakov-loop variables Φ, Φ^*, because there is only one minimum in the effective Polyakov-loop potential. However, the Polyakov-loop variables Φ, Φ^* will always develop their expectation values $\bar{\Phi}$ and $\bar{\Phi}^*$ in whole space, such that these fields should be regarded as homogeneous background thermal fields on top of which the chiral soliton is to be added.

IV. NONTOPOLOGICAL SOLITON SOLUTION IN THE MODEL

In vacuum, the Polyakov-loop variables Φ, Φ^* are set to zero and the thermodynamic grand potential $\Omega_{\rm MF}$ reduces to the purely mesonic potential $\Omega_{\rm M}$. Following Ref. [34], in the mean-field approximation, the σ and π are taken as time-independent, classical c-number fields, which only differ from their vacuum values in the neighborhood of the quark sources. The state of the quarks $\{\phi_n(\mathbf{r})\}$ with energy $\{\epsilon_n\}$ and the $\sigma(\mathbf{r})$, $\pi(\mathbf{r})$ meson fields satisfy the coupled set of the Euler-Lagrange equations of motion,

$$-i\vec{\alpha}\cdot\vec{\nabla}\phi_n(\mathbf{r}) - g\beta[\sigma(\mathbf{r}) + i\gamma_5\vec{\tau}\cdot\vec{\pi}(\mathbf{r})]\phi_n(\mathbf{r}) = \epsilon_n\phi_n(\mathbf{r}), \tag{18}$$

$$-\nabla^2\sigma(\mathbf{r}) + \frac{\partial\Omega_{\rm M}(\sigma_v)}{\partial\sigma} = -g\sum_{n_{\rm occ}}\bar{\phi}_n(\mathbf{r})\phi_n(\mathbf{r}), \tag{19}$$

$$-\nabla^2\vec{\pi}(\mathbf{r}) + \frac{\partial\Omega_{\rm M}(\sigma_v)}{\partial\vec{\pi}} = -g\sum_{n_{\rm occ}}\bar{\phi}_n(\mathbf{r})i\gamma_5\vec{\tau}\phi_n(\mathbf{r}), \tag{20}$$

with

$$\int\phi_n^\dagger(\mathbf{r})\phi_n(\mathbf{r})d^3r = 1, \tag{21}$$

where $\vec{\alpha}$ and β are the conventional Dirac matrices.

The ground state of the chiral soliton is the state with N quarks in the same lowest Dirac state ϕ_0, with energy ϵ. In the following, our discussions are constrained in the case of $N = 3$ for baryons. To obtain solutions of minimum energy, we adopt the "hedgehog" ansatz, where the meson fields are spherically symmetric and valence quarks are in the lowest s-wave level,

$$\sigma = \sigma(r), \quad \vec{\pi} = \hat{\mathbf{r}}\pi(r), \tag{22}$$

$$\phi_0 = \begin{pmatrix} u(r) \\ i\vec{\sigma}\cdot\hat{\mathbf{r}}v(r)\end{pmatrix}\chi, \tag{23}$$

where χ is a state in which the spin and isospin of the quark couple to zero:

$$(\vec{\sigma} + \vec{\tau})\chi = 0. \tag{24}$$

Now the system is spherical symmetric and the Euler-Lagrange equations of motion (18)–(20) transform in radial coordinates to

$$\frac{du(r)}{dr} = -[\epsilon + g\sigma(r)]v(r) - g\pi(r)u(r), \tag{25}$$

$$\frac{dv(r)}{dr} = -\left[\frac{2}{r} - g\pi(r)\right]v(r) + [\epsilon - g\sigma(r)]u(r), \tag{26}$$

$$\frac{d^2\sigma(r)}{dr^2}+\frac{2}{r}\frac{d\sigma(r)}{dr}-\frac{\partial\Omega_{\rm M}}{\partial\sigma}=Ng[u^2(r)-v^2(r)], \quad (27)$$

$$\frac{d^2\pi(r)}{dr^2}+\frac{2}{r}\frac{d\pi(r)}{dr}-\frac{2\pi(r)}{r^2}-\frac{\partial\Omega_{\rm M}}{\partial\pi}=-2Ngu(r)v(r), \quad (28)$$

and the quark functions should satisfy the normalization condition

$$4\pi\int r^2[u^2(r)+v^2(r)]dr=1. \quad (29)$$

These equations are subject to the boundary conditions which follow from the requirement of finite energy:

$$v(0)=0,\quad \frac{d\sigma(0)}{dr}=0,\quad \pi(0)=0, \quad (30)$$

$$u(\infty)=0,\quad \sigma(\infty)=f_\pi,\quad \pi(\infty)=0. \quad (31)$$

The asymptotic vacuum value of the soliton field has to be determined by an additional condition, i.e., that the physical vacuum is recovered at infinity. In this "physical" vacuum the quarks are free Dirac particles with the constituent mass $g\sigma_v$, and the chiral symmetry is spontaneously broken. By solving the coupled differential equations (25), (26), (27), and (28) with the normalization and the appropriate boundary conditions, in Fig. 4 we plot the σ, π, and quark fields profiles in arbitrary units as functions of r for zero temperature and chemical potential.

If we put N quarks into the lowest state with energy ϵ, the total energy of the hedgehog baryon is given by

$$E=N\epsilon+4\pi\int r^2\left[\frac{1}{2}\left(\frac{d\sigma}{dr}\right)^2+\frac{1}{2}\left(\frac{d\pi}{dr}\right)^2+\frac{\pi^2}{r^2}+\Omega_{\rm M}(\sigma_v)\right]dr, \quad (32)$$

which is normally identified as the mass of the nucleon M_N below.

As a next step we consider a $B=1$ localized bound state (soliton) in a thermal medium. Customarily, the thermal medium can be treated as a quark medium or a nuclear medium

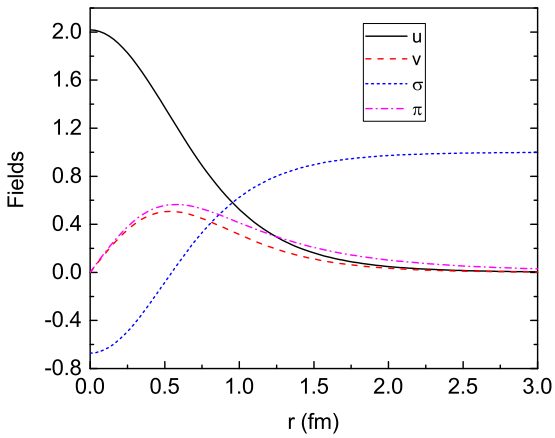

FIG. 4. The quark fields in relative units and the σ, π fields scaled with f_π as function of the radius r in vacuum.

owing to the interaction of the three valence quarks with the quark Dirac sea and the nucleon Fermi sea via the meson fields [51].

For the quark medium, the thermal medium is filled with quarks of a constituent mass M_q, and the soliton energy is given by the sum of the energy of the valence quarks, the meson fields, and their interactions as shown in Eq. (32). Then a new set of coupled equations of motion for the meson fields could be derived by simply replacing the relevant mesonic potential $\Omega_{\rm M}$ with the thermodynamic grand potential $\Omega_{\rm MF}$. Accordingly, a set of coupled equations for mesons can be described as

$$\frac{d^2\sigma(r)}{dr^2}+\frac{2}{r}\frac{d\sigma(r)}{dr}-\frac{\partial\Omega_{\rm MF}}{\partial\sigma}=Ng[u^2(r)-v^2(r)], \quad (33)$$

$$\frac{d^2\pi(r)}{dr^2}+\frac{2}{r}\frac{d\pi(r)}{dr}-\frac{2\pi(r)}{r^2}-\frac{\partial\Omega_{\rm MF}}{\partial\pi}=-2Ngu(r)v(r). \quad (34)$$

For satisfying the requirement of finite energy of the soliton, one of the boundary conditions in Eq. (31) should be modified accordingly as $r\to\infty$, $\sigma(r)$ approaches to the expectation value $\bar{\sigma}_v$, where thermodynamic grand potential $\Omega_{\rm MF}$ has an absolute minimum.

As long as the unbound constituent quarks, treated as the homogeneous background thermal fields with T and μ, are allowed to penetrate into the soliton, they will bring an additional contribution to the total baryon density. Thus, to ensure that the solitonic baryon number is equal to one, the normalization condition equation (29) should be modified as

$$4\pi\int r^2[u^2(r)+v^2(r)]dr=1-B_m, \quad (35)$$

with

$$B_m=4\pi\int_V\rho_B^m r^2dr. \quad (36)$$

Here $\rho_B^m=-\frac{1}{3}\frac{\partial\Omega_{\rm MF}}{\partial\mu}$ and V is the volume of the soliton.

In contrast, when a soliton is embedded in the medium of nucleons we have to consider a Fermi sea of nucleons instead of quarks, owing to confinement. This is because the Dirac sea consists of quarks and therefore only determines the vacuum sector. Thus, in this case the mesons are directly coupled to the nucleons of the Fermi sea. Accordingly, the terms representing the thermal medium effects in Eqs. (33) and (34) should be modified as

$$\frac{\partial\Omega_{\rm MF}}{\partial\sigma}\to g_N\langle\bar{\psi}_N\psi_N\rangle, \quad (37)$$

$$\frac{\partial\Omega_{\rm MF}}{\partial\pi}\to g_N\langle\bar{\psi}_N i\gamma_5\vec{\tau}\psi_N\rangle. \quad (38)$$

Here the bracket $\langle\ \ \rangle$ denotes the expectation value of the operator between the nuclear ground state, ψ_N is the nucleon field, and g_N is a coupling constant which relates the nucleon mass to the nonzero expectation value of the scalar meson field. Unluckily, both the coupling constant g_N and the scalar and pseudoscalar densities of nucleons and antinucleons in the above equations cannot be obtained from the present model

self-consistently. In fact, they have to be considered as input parameters which could be taken from the RMF approximation or the BHF theory [8,9]. Therefore, to avoid inconsistencies, it is customary to treat a hot and dense thermal medium as a uniform constituent quark and gluon medium (quark medium) with solitons embedded, as in Refs. [34,51,52].

As long as there is no baglike soliton solution for the Polyakov-loop variables Φ, Φ^* in whole space, the Polyakov-loop variables Φ, Φ^* take constantly their expectation values $\bar{\Phi}$ and $\bar{\Phi}^*$. Hence, these variables denote the contributions only to the thermodynamic grand potential $\Omega_{\rm MF}$ rather than to the equations of motion for the nontopological soliton solutions. Consequently, the properties of a soliton placed in a thermal medium can be investigated by solving the four coupled Euler-Lagrange equations that arise from the thermodynamic grand potential $\Omega_{\rm MF}$ in Eq. (15). This system of equations does not possess analytic solutions, but is readily solved numerically. Various numerical packages are available for the solution of such equations. One that has been widely used in this field is COLSYS [53].

V. NUCLEON STATIC PROPERTIES AT FINITE TEMPERATURE AND DENSITY

We first study soliton solutions at finite temperature and density by solving the coupled differential equations (25), (26), (33), and (34) with the normalization condition and the appropriate boundary conditions. In Fig. 5, we plot the $u(r)$, $v(r)$, $\sigma(r)$, and $\pi(r)$ fields at zero and finite chemical potential ($\mu = 380$ MeV) for different temperatures. These two chemical potentials correspond to the typical crossover and first-order phase transitions in the QCD phase diagram, respectively. For both cases, it is shown that all the fields are moving towards the trivial values while the temperature increases. When T is lager than some critical temperature T_χ^c, there only exist trivial solutions for the coupled equations of motion and solitons are melted away. These trivial solutions indicate the restoration of the chiral symmetry in full space. Moreover, the lack of solitonic solutions is usually considered as a signal for the delocalization of the baryonic phase.

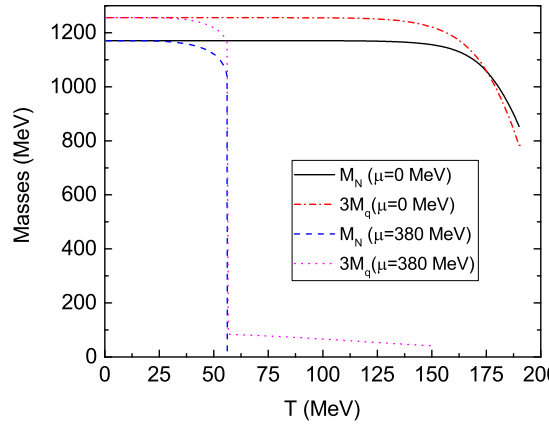

FIG. 6. The total energy of system M_N and the energy of three free constituent quark $3M_q$ as functions of temperature T. Here one set is for $\mu = 0$ MeV and another set is for $\mu = 380$ MeV.

Based on the above analysis, for both the crossover and first-order transitions the effective potential supports the existence of the stable soliton solution for the meson fields, as long as T is lower than T_χ^c. This implies that the baryonic phase can be indeed found in the chiral symmetry-breaking phase. However, the stability of such baryonic phase should be checked carefully by comparing the total energy of the system in the thermal medium with the energy of three free constituent quarks in the system. By subtracting the homogeneous medium contribution [34,51], the total energy of system M_N is plotted as a function of the temperature for $\mu = 0$ MeV and $\mu = 380$ MeV in Fig. 6. Here one finds that for a smooth crossover of the symmetry-breaking patten at the low-density region, both M_N and $3M_q$ fall smoothly from the corresponding vacuum value as T goes to high temperature. When T is close to some high critical temperature $T_\chi^c \simeq 201$ MeV for $\mu = 0$ MeV, both M_N and $3M_q$ experience a steep descent region. However, as shown in Fig. 6, in the high-temperature regime $3M_q$ drops more quickly than that of M_N, as $T > 177$ MeV, $3M_q < M_N$. This implies that even though the stable soliton solution still exists in the temperature region $T \in [177,201]$ MeV, it is energetically unfavorable.

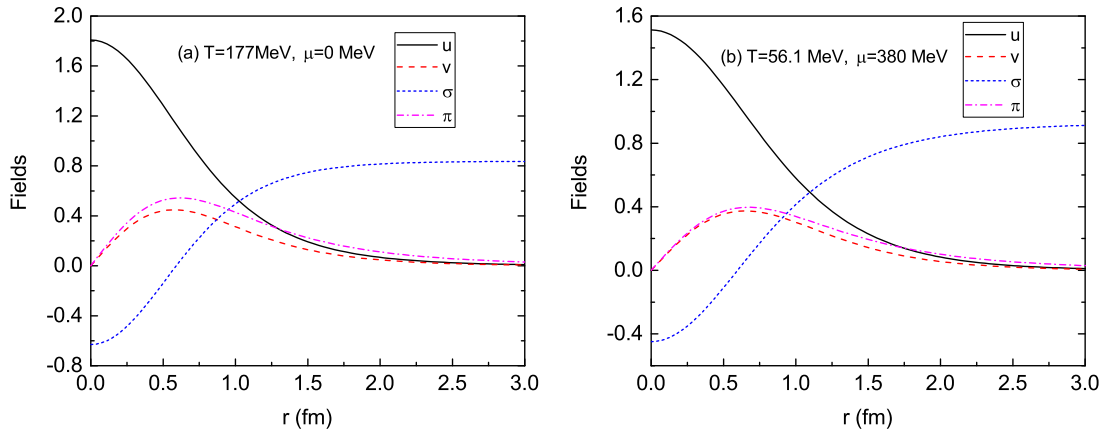

FIG. 5. (a) The quark fields in relative units and the σ, π fields scaled with f_π as function of the radius r for $T = 177$ MeV as $\mu = 0$ MeV. (b) The quark fields in relative units and the σ, π fields scaled with f_π as function of the radius r for $T = 56.1$ MeV, while $\mu = 380$ MeV.

The baryonic phase will definitely melt away into three free constituent quarks. In this way, we can identify this specific temperature $T_d^c \simeq 177$ MeV as a critical temperature of the deconfinement phase transition.

Based on the right panel in Fig. 6, one can see that in the large density region the total energy M_N decreases monotonically with increasing the temperature T from zero to higher values. As the temperature approaches the critical temperature T_χ^c, M_N starts to deviate from the ones in vacuum significantly. When $T > T_\chi^c$, M_N jumps to zero quickly, which indicates the delocalization phase transition from nucleon matter to quark matter owing to the fact that the effective potential does not support the existence of the stable soliton solution. The energy of three free constituent quark $3M_q$ (or σ_v) shows similar behavior as M_N. By comparing the two energies in Fig. 6, we can show that for $T < T_\chi^c$ the nucleon bound sate is stable and $3E_q$ is larger than M_N, but the difference decreases with the increase of temperature, and the two energies begin to cross over at the critical temperature T_χ^c. Therefore, the critical temperature for the deconfinement phase transition is coincident with that of the chiral phase transition for the first-order phase transition.

We infer the occurrence of the chiral phase transitions of u and d quarks and the deconfinement phase transition at finite temperature and finite density, and show the T-μ phase structure of the Polyakov quark-meson model in Fig. 7 based on the nontopological soliton picture. For two light flavors, there is a crossover in the low-density region and a first-order phase transition in the high-density region, and in the middle position there exists a CEP. From Fig. 7, the critical temperature for the deconfinement phase transition T_d^c is lower than that of the chiral phase transition, and both critical temperatures decrease smoothly as μ goes to high value. With the increasing of μ, the difference between T_χ^c and T_d^c becomes smaller and smaller, while at some critical chemical potential μ^c it becomes zero, which identifies the CEP for a second-order phase transition. The corresponding values are $(T^c, \mu^c) \simeq (119, 302)$ MeV.

Here are several remarks on the phase diagram presented in Fig. 7. From the above discussions on the effective potential and nontopological soliton concerning the deconfinement and chiral phase transition, we conclude that the effective potential always supports the existence of the stable soliton solution in the system if $T \leqslant T_\chi^c$, but not for $T > T_\chi^c$. It is required that the critical temperature defined as the deconfinement phase transition in a nontopological soliton model is usually less than the critical temperature for the chiral phase transition, as $T_d^c \leqslant T_\chi^c$. In this study, in the first-order region, we take the "=". In contrast, in the crossover region we should have the "<". This conclusion is in qualitative agreement with the result shown in Fig. 6 in Ref. [18] at relatively low and middle densities. However, for high density, they produce a very strange behavior for the deconfinement crossover phase transition for the Polyakov-loop variables Φ, Φ^*. This is different from the Friedberg-Lee model [37–39] and its descendant models [34,40], which only predict a first-order phase transition in the phase diagram. The chiral soliton model combined with the Polyakov loop has an obvious advantage in the description of QCD phase diagram, because it can allow the prediction of the crossover transition at low and middle chemical potentials. Nonetheless, it shows the first-order phase transition for high chemical potential. The result is in agreement with other predictions demonstrated in effective models and lattice QCD data [1–3].

At the end of this section, the proton charge rms radii R of a stable chiral soliton as a function of temperature for $\mu = 0$ MeV and $\mu = 380$ MeV are illustrated in Fig. 8; it gives a signal of a swelling of the nucleon when temperature and density increase. In both cases, R increases slightly at low temperatures while the latter is increased. As T approaches T_d^c,

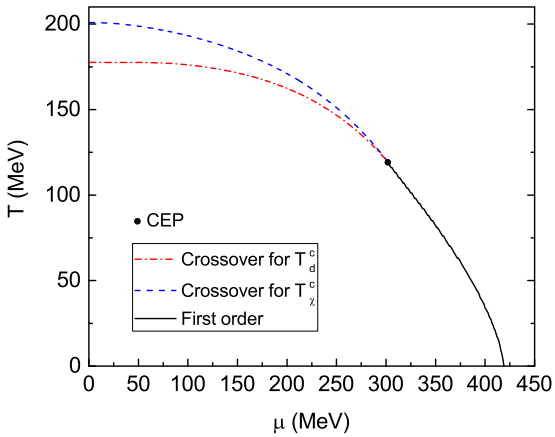

FIG. 7. Two-flavor phase diagram in the T-μ plane in the Polyakov quark-meson model based on the nontopological soliton picture. The dash-dotted curve is the critical line for T_d^c, which characterizes the confinement phase transition, and the dashed lines are the critical line for conventional chiral phase transition in the region of crossover. The solid lines indicate the first-order phase transitions, and the solid circle indicates the CEPs for chiral phase transitions of u and d quarks.

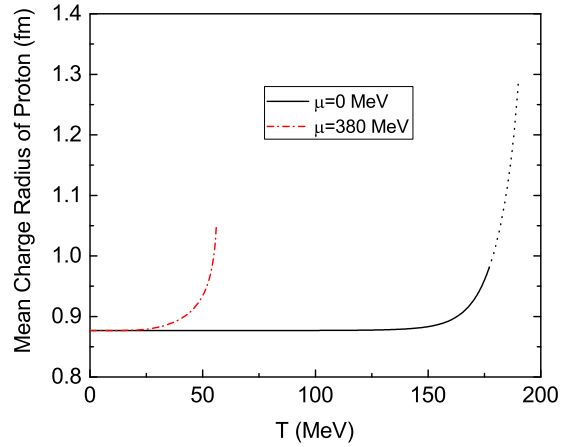

FIG. 8. The proton charge "rms" radius of a stable chiral soliton as a function of temperature T at $\mu = 0$ MeV and $\mu = 380$ MeV. The solid curve is for $\mu = 0$ MeV, while the dash-dotted curve is for $\mu = 380$ MeV. The dotted curve is for the unstable baryonic phase existing in the crossover phase transition when $T_\chi^c \geqslant T > T_d^c$.

R sharply grows and disappears. Another interesting result displayed in Fig. 8 is that the maximal radius R at various densities are almost the same when T is near T_d^c, which hints that solitons start to overlap each other with the similar expansion rate at T_d^c for different densities.

VI. QCD THERMODYNAMICS AT ZERO CHEMICAL POTENTIAL

To investigate the influence of the Polyakov loop on the equilibrium thermodynamics of the system, we calculate the pressure of the system P during the QCD phase transition form hadron phase to quark phase according to two different models as follows.

First, we adopt the mean-field approximation as usual by replacing σ, $\vec{\pi}$, and the Polyakov-loop variables Φ, Φ^* with their expectations values. In other words, we neglect both quantum and thermal fluctuations of the meson fields and the Polyakov-loop variables but retain the quarks and antiquarks as only quantum fields in the entire phase diagram. This is, of course, not a realistic scheme, especially at low T and μ, because, owing to the confining forces, quarks and antiquarks will recombine into mesons, baryons, and antibaryons. Hence, the character of the chiral phase transition described by the mean-field approximation could be drastically changed in hadronization process from quark phase to hadron phase. However, if we discard these affects, all thermodynamic quantities can be obtained from the grand-canonical potential in a spatially uniform system $\Omega_{\rm MF}$ in Eq. (15), which is determined as the logarithm of the partition function. The negative of grand potential which is normalized to vanish at $T = \mu = 0$ gives the thermodynamic pressure in the PQM model,

$$P_{\rm PQM} = -\Omega_{\rm MF}(T,\mu). \tag{39}$$

The pressure obtained in the above equation can be directly compared with lattice data.

However, the hadron and quark phases can be distinguished by empirical facts and phenomena at low and high energies. At low temperature and low baryon density, the hadronic phase exhibits a dynamical breaking of chiral symmetry and the confinement, and the baryon and meson act as the active degrees of freedom here. On the contrary, at very high temperature or baryon density, quarks and gluons will be set free to play the dominant roles in QGP. Such a scenario can be realized in the nontopological soliton (NS) model vividly as follows. In the hadron phase, the state of the free quarks is not the ground state of the strongly interacting matter, and as a result three valence quarks will form the bound state of the nucleon. Therefore, the hadron phase only possesses baryons and mesons. However, when $T > T_d^c$, the solitons are going to dissolve, and the hadronic phase will eventually evolve to quark phase with free quarks.

For simplicity, within the NS model, we assume an ideal case of the system by taking the hadronic phase as a noninteracting hadron gas composed of nucleons and π, σ mesons with the effective masses M_N, M_π, and M_σ in thermal medium. The Polyakov-loop variables are treated as the background thermal fields and, accordingly, the Polyakov-loop potential has been subtracted already. It is then straightforward to write the normalized pressure of the system in terms of nucleons and mesons for the hadronic phase [2,45],

$$\begin{aligned} P_{\rm NS}^{\rm H} = {} & \nu_N T \int \frac{d^3\vec{p}}{(2\pi)^3}\{\ln[1+e^{-(E_N-\mu_B)/T}]+\ln[1+e^{-(E_N+\mu_B)/T}]\} \\ & -\nu_\pi T \int \frac{d^3\vec{p}}{(2\pi)^3}\{\ln[1-e^{-E_\pi/T}]\} - \nu_\sigma T \int \frac{d^3\vec{p}}{(2\pi)^3}\{\ln[1-e^{-E_\sigma/T}]\} - B^*(M_N), \end{aligned} \tag{40}$$

where $\nu_N = 4$ for nucleon, $\nu_\pi = 3$ for pion, and $\nu_\sigma = 1$ for σ meson. The last term $B^*(M_N)$ is introduced to recover the thermodynamical consistency of the system, because the nucleons are treated as the chiral solitons with a temperature-dependent masses [54]. The explicit expression of this term can be evaluated by the additional constraint $(\partial P_{HP}/\partial M_N)_T = 0$, which gives

$$B^*[M_N(T)] = B^*[M_N(0)] - \nu_N \int_0^T dT' \frac{dM_N(T')}{dT'} M_N(T') \int \frac{d^3\vec{p}}{(2\pi)^3} \frac{1}{E'_N}\left[\frac{1}{e^{(E'_N-\mu_B)/T'}+1}+\frac{1}{e^{(E'_N+\mu_B)/T'}+1}\right], \tag{41}$$

with $E'_N = \sqrt{\vec{p}^2 + M_N(T')^2}$. The energies in Eq. (40) $E_N = \sqrt{\vec{p}^2 + M_N(T)^2}$, $E_\pi = \sqrt{\vec{p}^2 + M_\pi(T)^2}$, and $E_\sigma = \sqrt{\vec{p}^2 + M_\sigma(T)^2}$ are corresponding to nucleon, pion, and σ mesons, respectively. M_N is obtained as the energy of soliton, whereas the σ and π masses are determined by the curvature of $\Omega_{\rm MF}$ in Eq. (15) at the global minimum:

$$M_\sigma^2 = \frac{\partial^2\Omega_{\rm MF}}{\partial\sigma^2}, \quad M_\pi^2 = \frac{\partial^2\Omega_{\rm MF}}{\partial\pi^2}. \tag{42}$$

Because it is unfavorable for solitonic nucleons to survive at high energy when the temperature is across the deconfinement critical temperature $T_d^c \sim 177$ MeV, the baryonic bound state formed by three constituent quarks will definitely dissolve and the system should now be regarded as a quark phase including the free quarks, mesons and the gluons mimicked by the Polyakov loop. Consequently, the pressure of the NS model in terms of free quarks and mesons incorporating with the Polyakov-loop

potential in quark phase results in

$$P_{\rm NS}^{\rm Q} = \nu_q T \int \frac{d^3\vec{p}}{(2\pi)^3}\{\ln[1+e^{-(E_q-\mu)/T}]+\ln[1+e^{-(E_q+\mu)/T}]\} - \nu_\pi T \int \frac{d^3\vec{p}}{(2\pi)^3}\{\ln[1-e^{-E_\pi/T}]\}$$
$$- \nu_\sigma T \int \frac{d^3\vec{p}}{(2\pi)^3}\{\ln[1-e^{-E_\sigma/T}]\} - \mathcal{U}(\Phi,\Phi^*,T). \quad (43)$$

Here $\nu_q = 2N_cN_f = 12$ is the number of internal degrees of freedom of the quarks and $E_q = \sqrt{\vec{p}^2 + M_q^2}$ is the valence quark and antiquark energy for u and d quarks, and the constituent quark (antiquark) mass M_q is given by $M_q = g\vec{\sigma}_v$.

Thermodynamic pressures divided by the QCD Stefan-Boltzmann (SB) limit are illustrated at $\mu = 0$ MeV in Fig. 9 for three models, and the pressure has already been normalized to vanish at $T = \mu = 0$. For N_f massless quarks and $N_c^2 - 1$ massless gluons in the deconfined phase, the QCD pressure in the SB limit is given by

$$\frac{P_{\rm SB}}{T^4} = (N_c^2-1)\frac{\pi^2}{45} + N_cN_f\left[\frac{7\pi^2}{180} + \frac{1}{6}\left(\frac{\mu}{T}\right)^2 + \frac{1}{12\pi^2}\left(\frac{\mu}{T}\right)^4\right], \quad (44)$$

where the first term is the gluonic contribution and the rest involves the fermions.

At very high temperature, e.g., around twice the chiral critical temperature, the pressure of the PQM tends to approach that of the NS model in the quark phase. This implies that there only exists a weak interaction between particles in quark phase, and the quasiparticles model is a good approximation for the description of the weak-interaction QGP. However, when the temperature decreases, the $P_{\rm PQM}$ deviates from the pressure $P_{\rm NS}^{\rm Q}$ more and more. When the T reaches out to the chiral critical temperature $T_\chi^c \sim 201$ MeV, the gap between the two pressures arrives at its maximum value and then decrease smoothly until zero temperature is reached. For comparing with lattice simulations with a temporal extent of $N_\tau = 6$, which is closer to the continuum limit in Ref. [55], the strong interaction between the particles in the NS model cannot be simply discarded and it really plays a dominant role in producing a correct and reasonable thermodynamical pressure of the system.

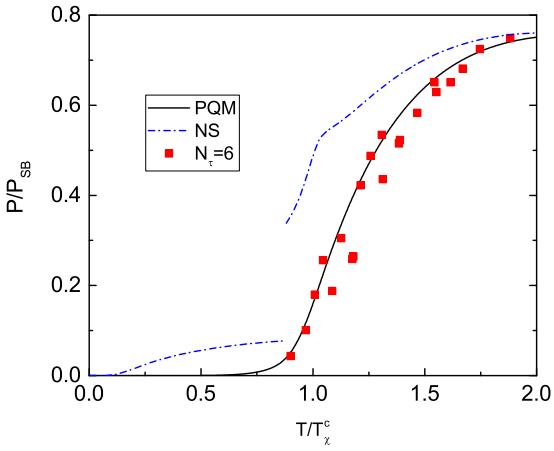

FIG. 9. The normalized pressure variations with respect to temperature for the PQM model and the NS model at $\mu = 0$, with $T_\chi^c \sim 201$ MeV. The solid line corresponds to the pressure in the PQM model, while the dash-dotted line is for the pressure in the NS model. All calculations are compared to lattice data ($N_\tau = 6$) from Ref. [55].

In Fig. 9, we also plot the pressure as a function of the temperature starting from the hadron to the quark phase at $\mu_B = 0$ for the NS model, while varying the baryon masses for various temperature and densities in the confined phase. From the figure, the dash-dotted curve shows rapidly changed discontinuities at the deconfinement critical temperature from hadron matter to quark matter. This indicates a pseudo-first-order phase transition for the delocalization transition and signals a drastic structural change for nucleons when the system goes with the diffusions of the solitons (nucleons) into thermal medium simultaneously. This strange behavior of the pressure $P_{\rm NS}$ around the deconfinement critical temperature T_χ^c is believed to be removed by bringing in a self-consistent interaction of σ, ω, ρ mesons with nuclear matter (solitons) in hadron phase. The strong interactions between mesons and nucleons, which are widely adopted in nuclear matter and finite nuclei [56–61], would provide necessary suppressions on the pressures for the mesons and nucleons in hadron phase, and the remaining self-interaction of the mesons in quark phase could give further suppression on the pressure around T_χ^c, similar to the PQM model. Finally, it is worth noting that, besides the interactions, another important influence which was neglected here is the center-of-mass (c.m.) correction to the nucleon properties, which have been considered in soliton bag models and the quark–meson coupling (QMC) model largely [61–64]. These two corrections are certainly out of the scope of our current topic and we prefer leaving them for a future study.

Unlike the case in the quark phase, here the pressures of the PQM model and the NS model are suppressed in the hadron phase and start to increase when deconfinement sets in. The small difference among the pressures of the $P_{\rm NS}$ and $P_{\rm PQM}$ is attributable to the different treatment of the mesons in the hadron phase. In the NS model the mesons are taken as the active degrees of freedom, but for the PQM model they are purely mean fields and should be restrained to the expectation values when T is close to the T_χ^c. From Fig. 6, it is shown that the effective nucleon mass M_N slightly deviates from its vacuum value with increasing temperature; only at the critical temperature T_χ^c does M_N experiences a sharp jump. Consequently, the contribution of nucleons to the total pressure in Eq. (40) is very small in hadron phase as far as the chemical potential is small. To estimate, it only gives 8.6% contribution

to $P_{\rm NS}$ when T is around $T_d^c \approx 177$ MeV for zero chemical potential. On the contrary, if three bound quarks are set to be free in quark phase, the valence quarks will give a dominant contribution to the pressure in Eq. (43).

VII. SUMMARY AND DISCUSSION

In the present paper we have investigated possible NS solutions in the effective potential of the PQM model in the presence of renormalized fermionic vacuum. The results show that as long as the temperature is not larger than the chiral critical temperature T_χ^c, there exist truly stable soliton solutions in the model for both crossover and first-order phase transitions.

Even though there are stable soliton solutions for the Euler-Lagrange equations of the model at finite temperature and density, the stability of the solitons (nucleons) have to be checked and analyzed carefully in thermal medium by comparing the effective masses of nucleons with the energies of three free constituent quarks. Our results show that the chiral phase transition and the delocalization phase transition from nucleon matter to quark matter take place simultaneously for the first-order phase transition. For $T < T_\chi^c$, the free constituent quarks are not the ground state of the strongly interacting system, and the quarks will reorganize so to form lower-energy bound states carrying the hedgehog configuration. However, as soon as the temperature T crosses over the T_χ^c, such bound states cannot survive anymore, and the system experiences a first-order hadron-quark phase transition to the chirally symmetric phase.

The situation differs from the case of the first-order transition, in the crossover transition, even though the effective potential genuinely ensures the stable soliton solution in the system, but it is energetically unfavorable for nucleons to exist when T is across the deconfinement critical temperature T_d^c. The difference between T_χ^c and T_d^c is about 24 MeV for zero chemical potential, but it will decrease to zero as μ increases to some value around 302 MeV. This particular point sometimes is denoted as the CEP, which appears as well in the phase diagram of Fig. 7.

To compare our results with the lattice QCD simulations and other models at zero chemical potential but finite temperature directly, we have investigated the thermodynamic properties of the NS model in the PQM model. It is found that the inclusion of the Polyakov loop is necessary and important when comparing with the lattice QCD simulations. When compared with the previous studies in this field, we notice quite an improvement on the topic by providing a reasonable critical deconfinement temperature $T_d^c \sim 177$ MeV for $\mu = 0$ and extracting a standard QCD phase diagram, in agreement with the lattice data and other phenomenological models' predictions [3]. However, the strange behavior of the performed pressure in the hadron-quark phase transition indicates that the description of the hadron phase as a noninteracting hadron gas of the nucleons and mesons with medium-modified masses has underestimated the important effects of their interactions, and these interactions should be introduced to further suppress the pressures of the mesons and nucleons in both hadron and quark phases. In other words, the present form of study is a prototype and still not suitable for the proper description of nuclear matter and finite nuclei in hadron phase yet, and it deserves further efforts on making the model applicable for hadron-quark phase transition completely and satisfactorily. Work in this direction is in progress.

ACKNOWLEDGMENTS

We thank Jingniu Hu for valuable comments and discussions. Authors are grateful to Professor Yijin Yan for his kind hospitality during our visit to Hong Kong University of Science and Technology. We are particularly grateful to Dr. Panagiotis Kotetes for his careful reading of the manuscript. The project is supported in part by National Natural Science Foundation of China (NSFC) under Grants No. 11274085 and No. 11275002.

[1] D. H. Rischke, Prog. Part. Nucl. Phys. **52**, 197 (2004).
[2] K. Yagi, T. Hatsuda, and Y. Miake, *Quark-Gluon Plasma: From Big Bang to Little Bang*, Cambridge Monographs on Particle Physics, Nuclear Physics and Cosmology, Vol. 23 (Cambridge University Press, Cambridge, England, 2008).
[3] K. Fukushima and T. Hatsuda, Rept. Prog. Phys. **74**, 014001 (2011).
[4] A. Chodos, R. L. Jaffe, K. Johnson, C. B. Thorn, and V. F. Weisskopf, Phys. Rev. D **9**, 3471 (1974); A. Chodos, R. L. Jaffe, K. Johnson, and C. B. Thorn, *ibid.* **10**, 2599 (1974); T. A. DeGrand, R. L. Jaffe, K. Johnson, and J. E. Kiskis, *ibid.* **12**, 2060 (1975).
[5] Y. Nambu and G. Jona-Lasinio, Phys. Rev. **122**, 345 (1961); **124**, 246 (1961).
[6] U. Vogl and W. Weise, Prog. Part. Nucl. Phys. **27**, 195 (1991); S. P. Klevansky, Rev. Mod. Phys. **64**, 649 (1992); T. Hatsuda and T. Kunihiro, Phys. Rep. **247**, 221 (1994); M. Buballa, *ibid.* **407**, 205 (2005).
[7] M. Gell-Mann and MLevy, Nuovo Cimento **16**, 705 (1960).
[8] P. Ring and P. Schuck, *The Nuclear Many-Body Problem* (Springer, Heidelberg, 1980).
[9] B. D. Serot and J. D. Walecka, *Advances in Nuclear Physics* (Plenum, New York, 1986), Vol. 16.
[10] N. Yasutake, T. Noda, H. Sotani, T. Maruyama, and T. Tatsumi, in *Recent Advances in Quarks Research*, edited by H. Fujikage (Nova Science, New York, 2013), Chap. 4, p. 63.
[11] O. Lourenco, M. Dutra, A. Delfino, and M. Malheiro, Phys. Rev. D **84**, 125034 (2011).
[12] G. Y. Shao, M. Di Toro, V. Greco, M. Colonna, S. Plumari, B. Liu, and Y. X. Liu, Phys. Rev. D **84**, 034028 (2011).
[13] P. Costa, M. C. Ruivo, C. A. de Sousa, and H. Hansen, Symmetry **2**, 1338 (2010), and references therein.
[14] T. K. Herbst, J. M. Pawlowski and B. J. Schaefer, Phys. Rev. D **88**, 014007 (2013).
[15] B. J. Schaefer, J. M. Pawlowski, and J. Wambach, Phys. Rev. D **76**, 074023 (2007).

[16] G. Marko and Z. Szep, Phys. Rev. D **82**, 065021 (2010).
[17] T. K. Herbst, J. M. Pawlowski, and B. J. Schaefer, Phys. Lett. B **696**, 58 (2011).
[18] U. S. Gupta and V. K. Tiwari, Phys. Rev. D **85**, 014010 (2012).
[19] V. Skokov, B. Friman, E. Nakano, K. Redlich, and B.-J. Schaefer, Phys. Rev. D **82**, 034029 (2010).
[20] V. K. Tiwari, Phys. Rev. D **86**, 094032 (2012).
[21] H. Mao, J. Jin, and M. Huang, J. Phys. G **37**, 035001 (2010).
[22] U. S. Gupta and V. K. Tiwari, Phys. Rev. D **81**, 054019 (2010).
[23] B. J. Schaefer, M. Wagner, and J. Wambach, Phys. Rev. D **81**, 074013 (2010).
[24] M. C. Birse and M. K. Banerjee, Phys. Lett. B **136**, 284 (1984); Phys. Rev. D **31**, 118 (1985).
[25] S. Kahana, G. Ripka, and V. Soni, Nucl. Phys. A **415**, 351 (1984).
[26] P. Alberto, E. Ruiz Arriola, M. Fiolhais, F. Grummer, J. N. Urbano, and K. Goeke, Phys. Lett. B **208**, 75 (1988).
[27] V. Bernard and U. G. Meissner, Nucl. Phys. A **489**, 647 (1988).
[28] P. Alberto, E. Ruiz Arriola, M. Fiolhais, K. Goeke, F. Grummer, and J. N. Urbano, Z. Phys. A **336**, 449 (1990).
[29] K. Goeke, M. Harvey, F. Grummer, and J. N. Urbano, Phys. Rev. D **37**, 754 (1988).
[30] T. S. T. Aly, J. A. McNeil, and S. Pruess, Phys. Rev. D **60**, 114022 (1999).
[31] C. V. Christov, E. Ruiz Arriola, and K. Goeke, Nucl. Phys. A **556**, 641 (1993).
[32] M. Abu-Shady and H. M. Mansour, Phys. Rev. C **85**, 055204 (2012).
[33] H. Chen, B. Liu, and H. Jiang, Chin. Phys. Lett. **14**, 645 (1997).
[34] H. Mao, T. Wei, and J. Jin, Phys. Rev. C **88**, 035201 (2013).
[35] H. Zhang, R. Dong, and S. Shu, Int. J. Mod. Phys. E **24**, 1550025 (2015).
[36] H. M. Mansour and M. Abu-Shady, J. Phys. G **43**, 025001 (2015).
[37] H. Reinhardt, B. V. Dang, and H. Schulz, Phys. Lett. B **159**, 161 (1985); H. Mao, M. Yao, and W.-Q. Zhao, Phys. Rev. C **77**, 065205 (2008).
[38] S. Gao, E. Wang, and J. Li, Phys. Rev. D **46**, 3211 (1992).
[39] M. Li, M. C. Birse, and L. Wilets, J. Phys. G **13**, 1 (1987).
[40] H. Mao, R.-K. Su, and W.-Q. Zhao, Phys. Rev. C **74**, 055204 (2006).
[41] K. Fukushima, Phys. Lett. B **591**, 277 (2004).
[42] A. M. Polyakov, Phys. Lett. B **72**, 477 (1978).
[43] C. Ratti, M. A. Thaler, and W. Weise, Phys. Rev. D **73**, 014019 (2006).
[44] O. Scavenius, A. Mocsy, I. N. Mishustin, and D. H. Rischke, Phys. Rev. C **64**, 045202 (2001).
[45] J. I. Kapusta and C. Gale, *Finite-temperature Field Theory: Principles and Applications* (Cambridge University Press, Cambridge, UK, 2006).
[46] K. A. Olive *et al.* (Particle Data Group Collaboration), Chin. Phys. C **38**, 090001 (2014).
[47] K. Fukushima, Phys. Rev. D **77**, 114028 (2008); **78**, 039902 (2008).
[48] R. Friedberg and T. D. Lee, Phys. Rev. D **15**, 1694 (1977); **16**, 1096 (1977); **18**, 2623 (1978).
[49] M. C. Birse, Prog. Part. Nucl. Phys. **25**, 1 (1990).
[50] R. Goldflam and L. Wilets, Phys. Rev. D **25**, 1951 (1982).
[51] J. Berger and C. V. Christov, Nucl. Phys. A **609**, 537 (1996).
[52] M. Schleif and R. Wunsch, Eur. Phys. J. A **1**, 171 (1998).
[53] U. Ascher, J. Christiansen, and R. D. Russell, ACM Trans. Math. Software **7**, 209 (1981).
[54] M. I. Gorenstein and S.-N. Yang, Phys. Rev. D **52**, 5206 (1995).
[55] A. Ali Khan *et al.* (CP-PACS Collaboration), Phys. Rev. D **64**, 074510 (2001).
[56] L. S. Celenza, A. Rosenthal, and C. M. Shakin, Phys. Rev. Lett. **53**, 892 (1984).
[57] M. Jandel and G. Peters, Phys. Rev. D **30**, 1117 (1984).
[58] W. Wen and H. Shen, Phys. Rev. C **77**, 065204 (2008).
[59] B. D. Serot and J. D. Walecka, Adv. Nucl. Phys. **16**, 1 (1986).
[60] P. A. M. Guichon, Phys. Lett. B **200**, 235 (1988).
[61] K. Saito, K. Tsushima, and A. W. Thomas, Prog. Part. Nucl. Phys. **58**, 1 (2007).
[62] I. Kimel, Phys. Rev. D **27**, 2129 (1983).
[63] E. G. Lubeck, M. C. Birse, E. M. Henley, and L. Wilets, Phys. Rev. D **33**, 234 (1986).
[64] E. G. Lubeck, E. M. Henley, and L. Wilets, Phys. Rev. D **35**, 2809 (1987).